# Analytical Methods

Accepted Manuscript


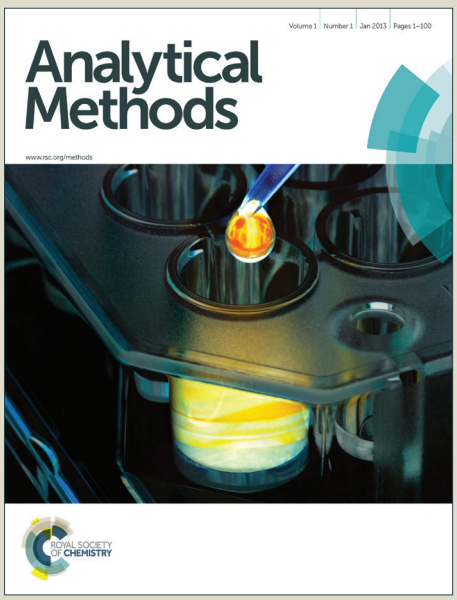





ROYAL SOCIETY OF CHEMISTRY

www.rsc.org/methods

# Highly-sensitive electrochemical sensor for simultaneous detection of Cd2+ and Pb2+ using liquid phase-exfoliated graphene

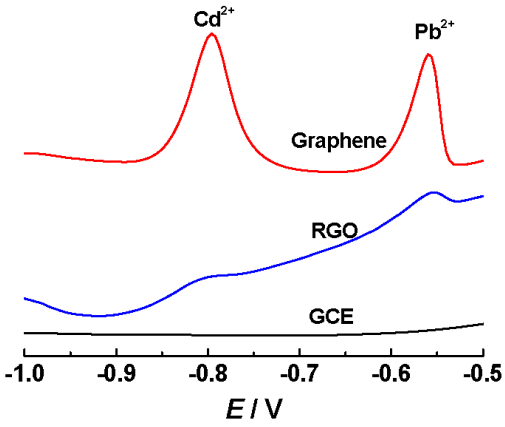

# Highly-sensitive electrochemical sensor for simultaneous detection of $Cd^{2+}$ and $Pb^{2+}$ using liquid phase-exfoliated graphene

Guishen Liu [a], Jianpeng Chen [a], Xiaodong Hou [a], Wensheng Huang [b*]

[a] *Chaozhou Quality and Measurement Supervision and Inspection Institute, Chaozhou 521011, China*

[b] *Key Laboratory of Biological Resources Protection and Utilization of Hubei Province, School of Chemistry and Environmental Engineering, Hubei Minzu University, Enshi 445000, China*

It is quite important to develop sensitive and simple analytical methods for toxic heavy metal ions, such as $Cd^{2+}$ and $Pb^{2+}$. Herein, liquid phase-exfoliated graphene nanosheets were easily prepared through one-step exfoliation of graphite powder in N-methyl-2-pyrrolidone. The obtained graphene suspension was directly used to modify the surface of glassy carbon electrode (GCE), constructing a novel and highly-sensitive electrochemical sensor for $Cd^{2+}$ and $Pb^{2+}$. Compared with the unmodified GCE and reduced graphene oxides-modified GCE, the resulting liquid phase-exfoliated graphene-modified GCE significantly increased the response signals of $Cd^{2+}$ and $Pb^{2+}$, showing remarkable signal amplification effects. The use of this defect abundant few layer graphene sample with small lateral flake sizes has lead to

* Corresponding author. E-mail: huang_wensh@163.com

the beneficial responses observed. The influences of supporting electrolyte, volume of graphene suspension, deposition potential and accumulation time were examined. As a result, a sensitive, rapid and convenient electrochemical method was developed for the simultaneous detection of $Cd^{2+}$ and $Pb^{2+}$. The detection limits were estimated to be 1.08 μg $L^{-1}$ and 1.82 μg $L^{-1}$ for $Cd^{2+}$ and $Pb^{2+}$. This new sensor was used in water sample analysis, and the results consisted with the values that obtained by inductively coupled plasma-atomic emission spectroscopy.

## Introduction

The monitoring of heavy ions, especially $Cd^{2+}$ and $Pb^{2+}$, has drawn wide attention because they are highly toxic and linked to various adverse health effects.[1,2] For example, environmental exposure to $Cd^{2+}$ increases the risk of cancer, and the international agency on cancer research has classified $Cd^{2+}$ as a carcinogen.[3] Therefore, developing sensitive, rapid and simple analytical methods for simultaneous determiantion of $Cd^{2+}$ and $Pb^{2+}$ is urgently needed. Compared with the widely-used atomic absorption spectroscopy (AAS), inductively coupled plasma-atomic emission spectroscopy (ICP-AES) and ICP-mass spectrometry (ICP-MS), electrochemical detection displays many advantages, such as good handling convenience, low cost, qualification for in-situ monitoring, and inexpensive equipments. Up-to-date, numerous electrodes have been developed for the simultaneous determination of $Cd^{2+}$ and $Pb^{2+}$.

Since its discovery, graphene, a novel two-dimensional carbon nanosheet, has received increasing attention and been widely used to modify electrode surface thanks to extraordinary properties such as large surface area, high catalytic activity, and strong accumulation ability.[4,5] Among these studies, graphene was almost prepared through chemical exfoliation of graphite using strong oxidizing reagents, especially according to Hummer's or modified Hummer's methods. However, preparation of graphen through chemical oxdaiton has some intrinsic drawbacks. For example, the procedure was complicated and rigorous, the intrinsic structure of graphite was likely to be destructed during chemical oxidation, and strong oxidizing reagents were largely consumed. Liquid phase exfoliation was proven to be an effective, mild and convenient approach to prepare graphene.[6,7] N-methyl-2-pyrrolidone (NMP) is an inexpensive organic solvent with low toxicity, and has been successfully used to exfoliate graphite to yield graphene nanosheets.[8,9] However, to the best of our knowledge, electrochemcial determiantion of $Cd^{2+}$ and $Pb^{2+}$ using graphene that prepared *via* liquid phase exfoliation has not been reported.

The main objective of this work was to develop a highly-sensitive electrochemical sensor for the simultaneous detection of $Cd^{2+}$ and $Pb^{2+}$ using liquid phase-exfoliated graphene as sensing film. Thus, graphene nanosheets were obtained by one-step exfoliation of graphite powder in NMP, and then used to modify electrode surface *via* solvent evaporation. The electrochemcial resposnes of $Cd^{2+}$ and $Pb^{2+}$ were studied using anodic stripping voltammetry. Compared with the widely-used reduced graphene oxides (RGO) prepared by chemical oxidation/reduction of graphite, the

resulting graphene significantly enhanced the stripping peak currents of $Cd^{2+}$ and $Pb^{2+}$. Undoubtedly, the obtained graphene is more active, and displays much higher sensitivity for the simultanesou detection $Cd^{2+}$ and $Pb^{2+}$.

## Experimental

### Reagents

All chemicals were of analytical grade and used as received. Graphite powder, NMP, $Cd^{2+}$ (1 mg $mL^{-1}$) and $Pb^{2+}$ (1 mg $mL^{-1}$) were obtained from the Sinopharm Group Chemical Reagent Co. Ltd (Shanghai China). Ultrapure water (18.2 MΩ) was obtained from a Milli-Q water purification system and used throughout.

### Instruments

Electrochemical measurements were performed on a CHI 660D electrochemical workstation (Chenhua Instrument, Shanghai, China). The working electrode was a glassy carbon electrode (GCE), the reference electrode was a saturated calomel electrode (SCE), and the counter electrode was a Pt wire. Scanning electron microscopy (SEM) measurements were conducted with a Quanta 200 microscope (FEI Company, Netherlands). Raman spectra was carried out on a LabRAM HR800 confocal Raman microscopy system using 532 nm laser (Horiba JobinYvon, France). $Cd^{2+}$ and $Pb^{2+}$ in water samples were also determined by ICP-AES (Perkin Elmer Optima model, 5300D, USA).

## Preparation of graphene-modified electrode

Graphene was prepared by ultrasonic exfoliation of graphite powder in NMP solvent. In a typical process, 0.25 g graphite powder was added into 50.0 mL NMP, and then sonicated in a KQ-100B ultrasonicator (frequency: 40 kHz, powder: 100 W) for 36 h. After 5-min centrifugation at 6000 rpm, the obtained suspension was used directly for the electrode modification.

For better comparison, graphene oxides (GO) and RGO were prepared through chemical oxidation and reduction methods.[10] Firstly, the graphite powders were oxidized by $H_2SO_4$, $K_2S_2O_8$ and $P_2O_5$ at 80 $^oC$ for 5 h, and the resulting products were reoxidized using concentrated $H_2SO_4$ and $KMnO_4$ in ice bath for 2 h. The mixture was filtered and washed with 10% HCl solution to remove metal ions. After being dried, the obtained GO samples were reduced to RGO using hydrazine.

Before modification, the glassy carbon electrode (GCE) with diameter of 3 mm was polished with 0.05 μm alumina slurry, and then sonicated in ultrapure water to give a clean surface. After that, 2 μL of the resulting graphene suspension was coated on GCE surface, and then dried under an infrared lamp in air. RGO and graphite powder were ultrasonically dispersed into water, and then used to modifiy GCE surface as controls through the above procedures.

## Analytical procedure

Unless otherwise stated, 0.1 M, pH 4.6 acetate buffer was used as supporting electrolyte for the determination of $Cd^{2+}$ and $Pb^{2+}$. The analysis includes accumulation

step and stripping step. Firstly, $Cd^{2+}$ and $Pb^{2+}$ were accumulated on the surface of liquid phase-exfoliated graphene-modified GCE, and then reduced to Cd and Pb under -1.0 V for 2 min. Subsequently, reduced Cd and Pb was oxidized to ions during the differential pulse sweep from -1.0 to -0.50 V, resulting in two sensitive stripping peaks at -0.80 V (for $Cd^{2+}$) and -0.56 V (for $Pb^{2+}$). The pulse amplitude was 50 mV, pulse width was 40 ms, and the scan rate was 40 mV $s^{-1}$.

## Results and discussion

### Characterization of prepared graphene

The surface morphology of bare GCE, graphite-modified GCE, RGO-modified GCE and prepared graphene-modified GCE was characterized using SEM. As seen in Fig. 1A, the surface of unmodified GCE was very smooth and virtually featureless. After modification with graphite, irregular and large particles were observed (Fig. 1B), suggesting poor dispersion abilities of graphite. On the surface of RGO-modified GCE (Fig. 1C) and liquid phase-exfoliated graphene-modified GCE (Fig. 1D), flexible and wrinkled nanosheets were clearly observed. Appearance of nanosheets indicates that the bulk graphite powder has been exfoliated to graphene. It is apparent that the flake sizes are smaller and this effectively gives rise to a greater edge plane content at this electrode in comparison to the others studied [11], thus it is likely that the small flake sizes will contribute to the beneficial response observed.

Fig. 2 depicts the Raman spectra of graphite powder and prepared graphene. Two obvious peaks at 1582 $cm^{-1}$ and 2700 $cm^{-1}$ were observed for the pristine graphite powder, which could be attributed to the natural G-band and 2D-band. For the prepared graphene, another notable peak at 1350 $cm^{-1}$ assigned to disorder-related D-band appeared. The D band shows the presence of edge plane like defects in the graphene sheet and instead it is largely recognised that the ratio between the G and 2D bands indicates the number of layers present in the graphene structure.[12] Through interpretation of these results it is suggested that the liquid-exfoliated graphene has few-layer (~>5 layers) with a large number of edge plane like surface defects (on the basal plane). It is inferred that this large edge plane content of the liquid exfoliated graphene is likely the origin of the beneficial electrochemical response.[13]

**Signal enhancement of graphene**

The electrochemical responses of $Cd^{2+}$ and $Pb^{2+}$ on GCE, RGO-modfieid GCE and obtained liquid phase-exfoliated graphene-modifeid GCE were compared to discuss the signal enhancement of graphene film. In pH 4.6 acetate buffer containing 50 μg $L^{-1}$ $Cd^{2+}$ and $Pb^{2+}$, the stipping curves on GCE surface were featureless, and no stripping peaks were observed after 2-min accumulation under -1.0 V (Fig. 3b). Clearly, the bare GCE exhibits very poor sensitivity for the detection of $Cd^{2+}$ and $Pb^{2+}$. When using RGO-modified GCE (Fig. 3d), two oxidation peaks with low sensitivity appeard at -0.80 V and -0.56 V for $Cd^{2+}$ and $Pb^{2+}$. This phenomenon indicates that RGO displays slight surface enhancement effects for $Cd^{2+}$ and $Pb^{2+}$. Graphene

nanosheets owns a much higher density of edge plane-like sites and defects, resulting in larger active areas and faster electron transfer.[11,14,15] Therefore, The response signals of $Cd^{2+}$ and $Pb^{2+}$ were improved on RGO surface. Interestingly, two greatly-increased oxdiaotn peaks were observed on the surface of liquid phase-exfoliated graphene-modified GCE (Fig. 3f). The peak potential differcence was as large as 240 mV, and the peak currents enhanced remarkably, revealing that the prepared graphene by liquid phase exfoliation exhibits very strong signal enhancement for $Cd^{2+}$ and $Pb^{2+}$. Compared with RGO, graphene prepared by liquid phase exfoliation possesses more global coverage of electrochemically reactive edge plane sites and defects, which in turn is expected to result in the increased electrochemical reactivity of the electrode.[13,16] As a result, the stripping peak currents of $Cd^{2+}$ and $Pb^{2+}$ were further increased obviously on the prepared graphene-modified electrode. In the absence of $Cd^{2+}$ and $Pb^{2+}$, the stripping curves on GCE (Fig. 3a), RGO-modified GCE (Fig. 3c), and liquid phase-exfoliated graphene-modified GCE (Fig. 3e) became smooth and featureless. So the oxidation peaks in Fig. 3 were attributed to $Cd^{2+}$ and $Pb^{2+}$. In conclusion, graphene prepared by liquid phase exfoliation is more acitve for the simultaneous detection of $Cd^{2+}$ and $Pb^{2+}$, and certainly increases the detection sensitivity greatly.

**Simultaneous detection of $Cd^{2+}$ and $Pb^{2+}$**

The anodic stripping responses of $Cd^{2+}$ and $Pb^{2+}$ in 0.1 M acetate buffer with different pH values, such as 3.6, 4, 4.6, 5 and 5.6, were studied, and the results were

shown in Fig. 4. With gradual improvement of pH value from 3.6 to 4.6, the stripping peak currents of $Cd^{2+}$ and $Pb^{2+}$ on the graphene-modified GCE enhanced considerably. As further improving pH value from 4.6 to 5.6, the stripping peak currents of $Cd^{2+}$ and $Pb^{2+}$ gradually decreased. Clearly, the response signals of $Cd^{2+}$ and $Pb^{2+}$ on the graphene-modified GCE were highest at pH of 4.6.

The influences of surface amount of graphene were examined on the stripping peak currents of $Cd^{2+}$ and $Pb^{2+}$. As illustrated in Fig. 5, the stripping peak currents of $Cd^{2+}$ and $Pb^{2+}$ increased remarkably with improving the volume of graphene suspension from 0 to 2 μL. During this period, the increrased graphene on GCE surface obviously enhanced the accumulation ability for $Cd^{2+}$ and $Pb^{2+}$, resulting in notable peak currents enhancement. After that, the stripping peak currents of $Cd^{2+}$ and $Pb^{2+}$ decreased slightly as further increaseing the volume of graphene suspension. For higher sensitivity and shorter time for solvent evaporation, 2 μL graphene suspension was used for the detection of $Cd^{2+}$ and $Pb^{2+}$.

The effects of accumulation potential and time were also studied because these two parameters affected the detection sensitivity to some extent. Fig. 6 shows the influences of accumulation potential on the stripping peak current of $Cd^{2+}$ and $Pb^{2+}$. It was found that the stripping peak currents of $Cd^{2+}$ and $Pb^{2+}$ increased rapidly with shifting accumulation potential from -0.8 V to -0.9 V. At more negative potential, accumulated $Cd^{2+}$ and $Pb^{2+}$ is reduced more completely. Thus, the resulting oxidation signals enhance remarkably. When the accumulation potential moved from -0.9 V to -1.2 V, the stripping peak currents of $Cd^{2+}$ and $Pb^{2+}$ almost kept unchanged, indicating

that a limiting reduction potential was achieved. However, the stripping peak currents began to decrease and the background currents enhanced obviously when the accumulation potential was lower than -1.2 V. More negative accumulation potential will lead other metal ions or $H^+$ to be reduced, causing interference for the determination of $Cd^{2+}$ and $Pb^{2+}$. Therefore, the optimized accumulation potential was controlled at -1.0 V.

Fig. 7 displays the effects of accumulation time on the deetction sensitivity of $Cd^{2+}$ and $Pb^{2+}$. By extending the accumulation time from 0.5 to 2 min, the stripping peak currents of $Cd^{2+}$ and $Pb^{2+}$ increased greatly. A longer accumulation time will cause more and more ions to be accumulated on the surface of liquid phase-exfoliated graphene-modified GCE. Consequently, the stripping peak currents also enhance significantly. When we extended the accumulation time from 2 to 5 min, the degree of peak current enhancement gradually decreased. Considering sensitivity and working efficiency, 2-min accumulation was employed.

**Analytical properteis for $Cd^{2+}$ and $Pb^{2+}$**

Because of strong adsorption, $Cd^{2+}$ and $Pb^{2+}$ is difficult to escape from the surface of graphene. Therefore, the liquid phase-exfoliated graphene-modified GCE was just used for single measurement. The reproducibility between multiple electrodes was estimated by comparing the stripping peak currents of 50 μg $L^{-1}$ $Cd^{2+}$ and $Pb^{2+}$. The vauels of relative standard deviation (RSD) of twelve graphene-modified GCEs were 3.2% for $Cd^{2+}$ and 4.3% for $Pb^{2+}$, suggesting good

fabrication reproducibility and detection precision.

The potential interferences of other metal ions on the detection of 50 μg $L^{-1}$ $Cd^{2+}$ and $Pb^{2+}$ were evaluated under the optimized conditions. It was found that 0.1 M $Ca^{2+}$, $Mg^{2+}$, $Al^{3+}$, $Zn^{2+}$, $Mn^{2+}$; 0.01 M $Ni^{2+}$, $Fe^{3+}$; and 0.01 mM $Hg^{2+}$, $Bi^{3+}$; did not interfere with the stripping peak currents of $Cd^{2+}$ and $Pb^{2+}$.

The linear range and detection limit were also evaluated under the optimized conditions. As shown in Fig. 8, the stripping peak current ($I_p$, μA) increased linearly with the concentration ($C$, μg $L^{-1}$) over the range from 2.5 to 100 μg $L^{-1}$. The linear regression quations were $I_p = 0.204\ C$ (for $Cd^{2+}$) and $I_p = 0.169\ C$ (for $Pb^{2+}$). The correlation coefficients were higher than 0.997, indicative of good linearity. After 2-min accumulation, the values of detection limit were calculated to be 1.08 μg $L^{-1}$ and 1.82 μg $L^{-1}$ for $Cd^{2+}$ and $Pb^{2+}$ based on three signal-to-noise ratio.

## Practical application

In order to evaluate the practical application of this new sensor, it was used to determine $Cd^{2+}$ and $Pb^{2+}$ in different water samples. The samples were filtered using a 0.45 μm filter membrane before analysis. After adding 5.0 mL sample solution into 5.0 mL pH 4.6 acetate buffer, the differential pulse voltammograms were recorded from -1.0 V to -0.3 V after 2-min accumulation. Each sample underwent three parallel detections, and the values of RSD were below 5%, indicating good precision. The concentration of $Cd^{2+}$ and $Pb^{2+}$ was obtained by standard addition method, and the results were listed in Table 1. Additionally, ICP-AES was also used to testify the

accuracy of this sensor. It was found that the obtained results were in good agreements, and the relative error was below 6%, revealing that the newly-developed method is accurate and has promising application.

## Conclusions

Graphene was easily obtained *via* one-step ultrasonic exfoliation of graphite powder in NMP solvent, and then used to construct a highly-sensitive sensing film for $Cd^{2+}$ and $Pb^{2+}$. Owing to larger response area and high adsorption ability, the liquid phase-exfoliated graphene-modified elecrode greatly enhanced the stripping peak currents of $Cd^{2+}$ and $Pb^{2+}$, as well as the detection sensitivity. From the comparison that listed in Table 2, it was apparent that this new sensor exhibited higher sensitivity compared with the reported electrochemical sensors. In addition, this new method for simultaneous detection of $Cd^{2+}$ and $Pb^{2+}$ dispalyed great potential in practical sample analysis because of good accuracy.

## Acknowledgements

This work was supported by the National Natural Science Foundation of China (Nos. 61361009), the Research Project of General Administration of Quality Supervision, Inspection and Quarantine of China (2013Qk279), the Open Foundation of Key Laboratory of Biologic Resources Protection and Utilization of Hubei Province (PKLHB PKLHB1313), and Project of New Strategic Industries for

Fostering Talents in Applied Chemistry of Higher Education of Hubei Province, China.

## References

1 B. Nowak and J. Chmielnicka, *Ecotox. Environ. Safe.*, 2000, **46**, 265-274.

2 X.B. Feng, P. Li, G. Qiu, S.F. Wang, G.H. Li, L.H. Shang, B. Meng, H.M. Jiang, W.Y. Bai, Z.G. Li and X.W. Fu, *Environ. Sci. Technol.*, 2008, **42**, 326-332.

3 T. Nawrot, M. Plusquin, J. Hogervorst, H.A. Roels, H. Celis, L. Thijs, J. Vangronsveld, E.V. Hecke and J.A. Staessen, *The Lancet Oncol.*, 2006, **7**, 119-126.

4 Y.Q. Zhang, Y.Z. Wang, J.B. Jia and J.G. Wang, *Sens. Actuator B-Chem.*, 2012, **171**, 580-587.

5 C.Wu, D. Sun, Q. Li and K.B. Wu, *Sens. Actuator B-Chem.*, 2012, **168**, 178-184.

6 D. Nuvoli, L. Valentini, V. Alzari, S. Scognamillo, S.B. Bon, M. Piccinini, J. Illescas and A. Mariani, *J. Mater. Chem.*, 2011, **21**, 3428-3431.

7 K.H. Park, B.H. Kim, S.H. Song, J. Kwon, B.S. Kong, K. Kang and S. Jeon, *Nano Lett.*, 2012, **12**, 2871-2876.

8 Y. Hernandez, V. Nicolosi, M. Lotya, F.M. Blighe, Z.Y. Sun, S. De, I.T. Mcgovern, B. Holland, M. Byrne, Y.K. Gun'ko, J.J. Boland, P. Niraj, G. Duesberg, S. Krishnamurthy, R. Goodhue, J. Hutchison, V. Scardaci, A.C. Ferrari and J.N. Coleman, *Nat. Nanotechnol.*, 2008, **3**, 563-568.

9 C. Wu, Q. Cheng, L.Q. Li, J.P. Chen and K.B. Wu, *Electrochim. Acta*, 2014, **115**, 434-439.

10 D. Li, M.B. Müller, S. Gilje, R.B. Kaner and G.G. Wallace, *Nat. Nanotechnol.*, 2008, **3**, 101-105.

11 D.A.C. Brownson, L.J. Munro, D.K. Kampouris and C. E. Banks, *RSC Adv.*, 2011, ***1***, 978-988.

12 U. Khan, A. O'Neill, M. Lotya, S. De, and J. N. Coleman, *Small*, 2010, **6**, 864-871.

13 D.A.C. Brownson, S.A. Varey, F. Hussain, S.J. Haigh and C.E. Banks, *Nanoscale*, 2014, **6**, 1607-1621.

14 D.A.C. Brownson, D.K. Kampouris and C.E. Banks, *Chem. Soc. Rev.*, 2012, **41**, 6944-6976.

15 L.C.S. Figueiredo-Filho, D.A.C. Brownson, O. Fatibello-Filho and C. E. Banks, *Analyst*, 2013, **138**, 4436-4442.

16 L.C.S. Figueiredo-Filho, D.A.C. Brownson, M. Gómez-Mingot, J. Iniesta, O. Fatibello-Filho and C.E. Banks, *Analyst*, 2013, **138**, 6354-6364.

17 D.S. Rajawat , A. Kardam and S. Srivastava, *Environ. Sci. Pollut. Res.*, 2013, **20**, 3068-3076.

18 M. Malisic, A. Janosevic, B. Paunkovic, I. Stojkovic and G. Marjanovic, *Electrochim. Acta*, 2012, **74**, 158-164.

19 J. Saturno, D. Valera, H. Carrero and L. Fernández, *Sens. Actuator B-Chem.*, 2011, **159**, 92-96.

20 G. Lee, C.K. Kim, M.K. Lee and C.K. Rhee, *Electroanalysis*, 2010, **22**, 530-535.

21 C.Z. Zhao, H. Liu and L. Wang, *Anal. Methods*, 2012, **4**, 3586-3592.

22 E. Svobodova-Tesarova, L. Baldrianova, M. Stoces, I. Svancara, K. Vytras, S.B. Hocevar and B. Ogorevc, *Electrochim. Acta*, 2011, **56**, 6673-6677.

23 Z.M. Wang, E.J. Liu and X. Zhao, *Thin Solid Films*, 2011, **519**, 5285-5289.

24 E.A. McGaw and G.M. Swain, *Anal. Chim. Acta*, 2006, **575**, 180-189.

25 X. Guo, Y. Yun, V.N. shanov, H.B. Halsall and W.R. Heineman, *Electroanalysis*, 2011, **23**, 1252-1259.

26 G. Kefala and A. Economou, *Anal. Chim. Acta*, 2006, **576**, 283-289.

## Captions for figrues and tables

Fig. 1 SEM images of GCE (A) , graphite-modified GCE (B), RGO-modified GCE (C)and liquid phase-exfoliatedgraphene-modified GCE (D).

Fig. 2 Raman spectra of graphite and liquid phase-exfoliated graphene.

Fig. 3 Anodic stripping curves of 50 μg $L^{-1}$ $Cd^{2+}$ and $Pb^{2+}$ on GCE (b), RGO-modifeid GCE (d) and liquid phase exfoliated graphene-modified GCE (f). (a, c, e): corresponding blank curves. Accumulation potential: -1.0 V, time: 2 min, amount of suspension: 2 μL.

Fig. 4. Effects of pH value on the stripping peak currents of 50 μg $L^{-1}$ $Cd^{2+}$ and $Pb^{2+}$ on liquid phase-exfoliated graphene-modified GCE. Other conditions were the same as in Fig. 3.

Fig. 5 Influences of amount of graphene suspension on the stripping peak currents of 50 μg $L^{-1}$ $Cd^{2+}$ and $Pb^{2+}$. Other conditions were the same as in Fig. 3

Fig. 6 Variation of stripping peak currents of 50 μg $L^{-1}$ $Cd^{2+}$ and $Pb^{2+}$ as a function of accumulation potential. Other conditions were the same as in Fig. 3.

Fig. 7 Effects of accumulation time on the stripping peak currents of 50 μg $L^{-1}$ $Cd^{2+}$ and $Pb^{2+}$. Other conditions were the same as in Fig. 3.

Fig. 8A Anodic stripping curves of $Cd^{2+}$ and $Pb^{2+}$ on liquid phase-exfoliated graphene-modified GCE with different concentrations of 0 (a), 2.5 (b), 10 (c), 20 (d), 30 (e), 40 (f), 50 (g), 80 (h) and 100 μg $L^{-1}$ (i). Fig. 8B Calibration curves of $Cd^{2+}$ and $Pb^{2+}$. Accumulation potential: -1.0 V, time: 2 min, amount of graphene suspension: 2 μL.

Table 1 Detection of $Cd^{2+}$ and $Pb^{2+}$ in water samples.

Table 2 Comparison of electrochemical sensors for $Cd^{2+}$ and $Pb^{2+}$.

Fig. 1

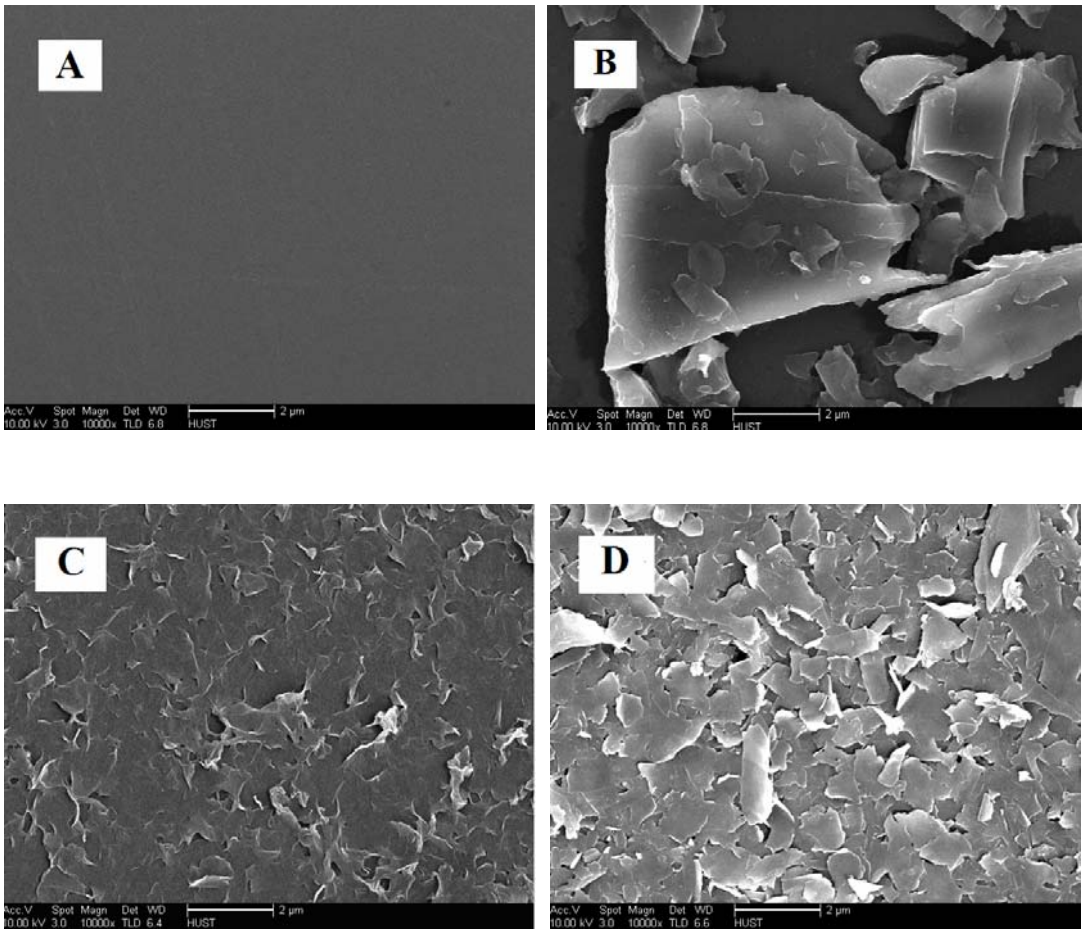

Fig. 2

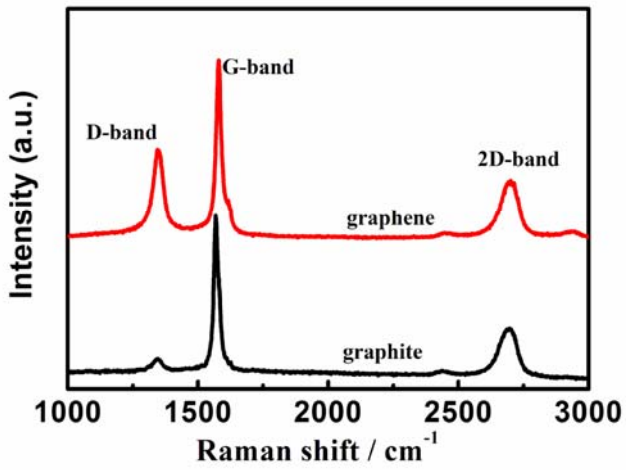

Fig. 3

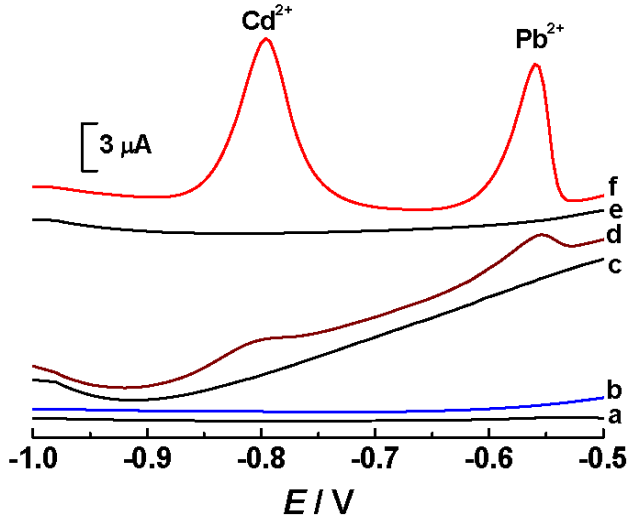

Fig. 4

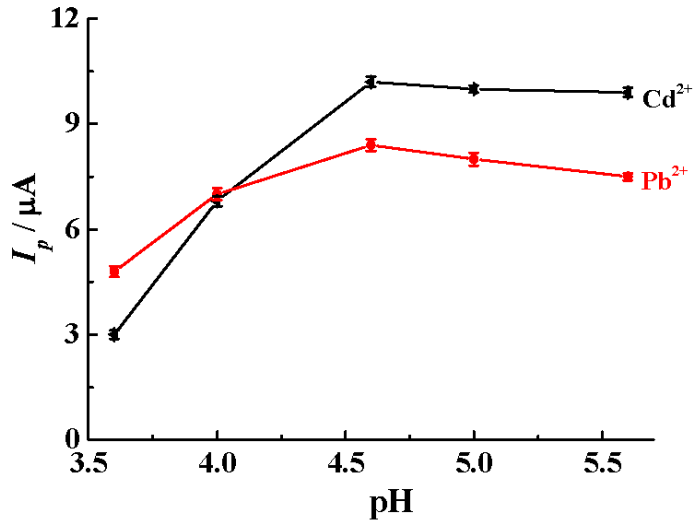

Fig. 5

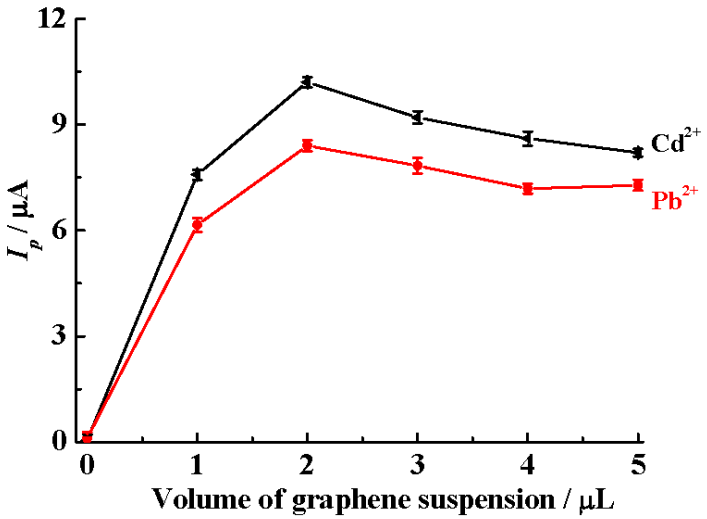

Fig. 6

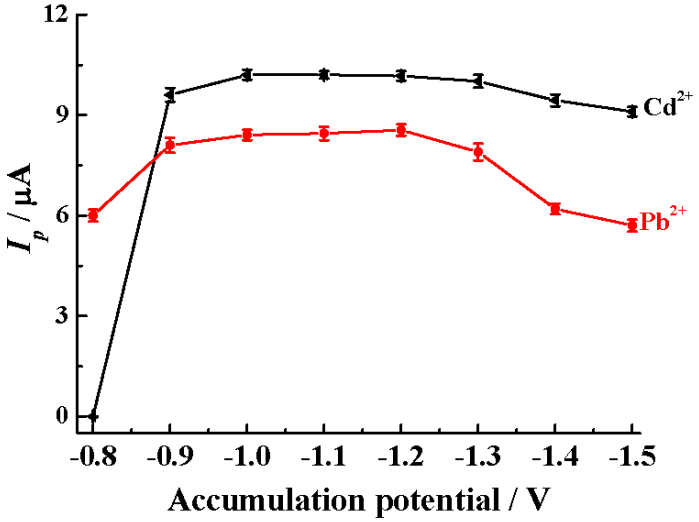

Fig. 7

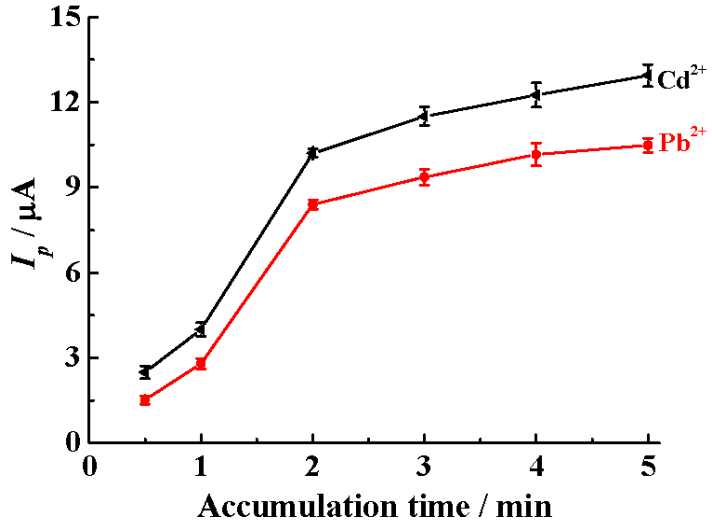

Fig. 8

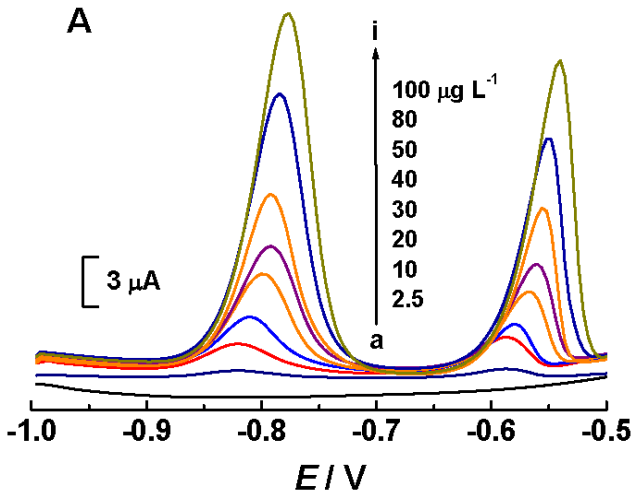


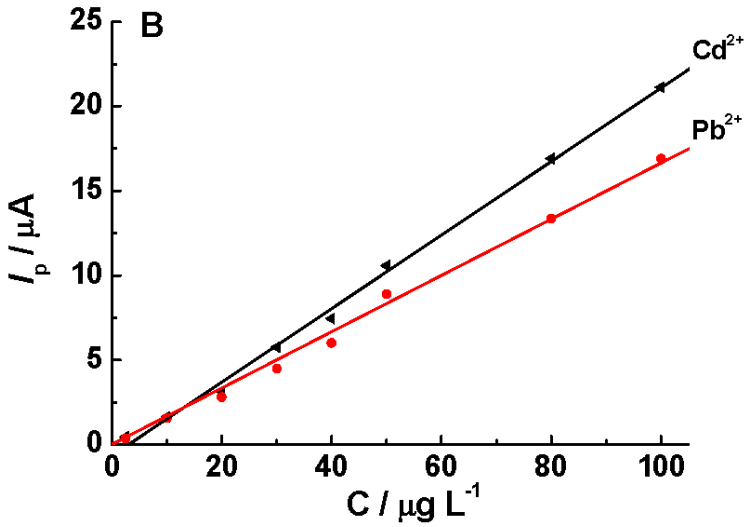

Table 1 Detection of $Cd^{2+}$ and $Pb^{2+}$ in water samples.

| Sample | Analyte | By this sensor ($\mu g\ L^{-1}$) | By ICP-AES ($\mu g\ L^{-1}$) | Relative error |
|---|---|---|---|---|
| A | $Cd^{2+}$ | 21.46 | 20.67 | 3.8% |
| | $Pb^{2+}$ | 11.24 | 10.81 | 4.0% |
| B | $Cd^{2+}$ | 32.56 | 33.89 | -3.9% |
| | $Pb^{2+}$ | 22.07 | 21.29 | 3.7% |
| C | $Cd^{2+}$ | 17.36 | 18.45 | -5.9% |
| | $Pb^{2+}$ | 27.83 | 26.42 | 5.3% |
| D | $Cd^{2+}$ | 75.12 | 77.74 | -3.4% |
| | $Pb^{2+}$ | 53.47 | 55.71 | -4.1% |

Table 2 Comparison of electrochemical sensors for $Cd^{2+}$ and $Pb^{2+}$.

| Sensing materials | Detection limit for $Cd^{2+}$ /μg $L^{-1}$ | Detection limit for $Pb^{2+}$ /μg $L^{-1}$) | Time /min | Ref. |
|---|---|---|---|---|
| Nanocellulosic fiber | 88 | 33 | 10 | 17 |
| $MnO_2$-carbon composites | 5.85 | 5.60 | 2 | 18 |
| Nanostructured bismuth | 11 | 18 | 2 | 19 |
| Bismuth Nanopowder | 4.2 | 2.54 | 10 | 20 |
| Electropolymerized thiadiazole film | 50 | 300 | 5 | 21 |
| Antimony powder | 1.4 | 0.9 | 2 | 22 |
| Polyaniline film | 14.6 | 20.72 | 2 | 23 |
| boron-doped diamond | 1 | 5 | 3.5 | 24 |
| Carbon nanotube | 2.81 | 2.47 | 2 | 25 |
| Polymer-coated bismuth film | 2 | 2 | 2 | 26 |
| Graphene prepared by liquid phase exfoliation | 1.08 | 1.82 | 2 | This work |